Microrheology with Optical Tweezers: Peaks & Troughs

Manlio Tassieri

Division of Biomedical Engineering, School of Engineering, University of Glasgow, Glasgow G12 8LT, UK

Abstract

Since their first appearance in the '70s, Optical Tweezers have been successfully exploited for a variety of applications throughout the *natural sciences*, revolutionising the field of micro-sensing. However, when adopted for microrheology studies, there exist some *peaks & troughs* on their *modus operandi* and data analysis that I wish to address and possibly iron out, providing a guide to future rheological studies from a microscopic perspective.

Keywords: Microrheology, optical tweezers, complex fluids, viscoelasticity

1. Introduction

In the '70s, a team of researchers led by Arthur Ashkin (the co-winner of the 2018 Nobel Prize in Physics) developed [1, 2, 3] what has revealed to be an invaluable tool for a myriad of investigations throughout the *natural sciences* [4] •[5] •[6] •[7] •[8] •[9]: "*Optical Tweezers*" (OT). Their success relies on the inherent property that a highly focused laser beam has to weakly trap (in three dimensions) micron-sized dielectric objects suspended into a fluid. OT have proved to be exceptionally sensitive transducers capable of resolving 'pN' forces and 'nm' displacements with a high temporal resolution; i.e. down to a few 'μsec', reshaping the field of micro-sensing •[10] •[11] •[12] •[13]. Therefore, they have been promptly adopted to study a myriad of biological processes,

Email address: Manlio.Tassieri@glasgow.ac.uk (Manlio Tassieri)

such as trapping otoliths in larval zebrafish • [14], measuring the forces exerted by a single motor protein ••[15], the mechanical properties of human red blood cells •• [16] and those of individual biological molecules •[17]•[18]•[19]; normally inaccessible by conventional methods.

Accessing the time-dependent trajectory of a micron-sized sphere, to a high spatial and temporal resolution, is one of the principles underpinning microrheology techniques [20, 21]. Microrheology is a branch of *rheology* (the study of flow of matter) and it is underpinned by the same principles, but it works at micron length scales and with micro-litre sample volumes. Therefore, microrheology techniques have revealed to be very useful methods for all those rheological studies where 'rare' or 'precious' materials are employed, e.g. in biophysical studies [22, 23, 24, 25, 26, 27, 28]. Moreover, microrheology measurements can be performed *in situ* in an environment that cannot be reached by a conventional rheology experiment, for instance inside a living cell [29, 30]. The most popular microrheology techniques are: video particle tracking microrheology [31], diffusing wave spectroscopy [32, 33], dynamic light scattering [34, 35], atomic force microscopy [36, 37], magnetic tweezers [38, 22] and optical tweezers [39, 40, 41, 42, 43, 44, 45, 46, 47]. These are classified as either 'active' or 'passive' techniques, depending on whether the particle displacement is induced by an external force field or generated by the thermal fluctuations of the fluid molecules surrounding the probe particle, respectively. For a good overview and understanding of the historical roots of the most common microrheology techniques, the reader is referred to Refs. [48, 49, 21, 50, 51].

A common task of microrheology studies is to correlate the time-dependent trajectories of the tracer particles to the frequency-dependent linear viscoelastic (LVE) properties of the suspending fluid. In the specific case of OT, methods for performing linear microrheology measurements of complex fluids have been presented [43, 44, 52] and validated [52, 53, 27, 54] against conventional bulk rheology methods. However, in literature there exist some '*peaks & troughs*' (not to mention inconsistencies) on the *modus operandi* of microrheology measurements performed with OT that I wish to address and possibly 'iron out'

avoiding future potentially misleading outcomes. In particular, in the following sections, after a brief introduction to the underlying principles of linear rheology, I provide a critical overview of all those experimental and data analysis aspects that, if overlooked or miscalculated, may compromise the quality of the outputs of 'linear' microrheology measurements with OT. In the case of non-linear microrheology with OT, I refer the reader to a recent review presented by Robertson-Anderson ••[55] and those there in.

2. Theoretical background

2.1. Linear rheology

The linear viscoelastic properties of a generic material can be expressed in terms of its shear complex modulus $G^*(\omega) = G'(\omega) + iG''(\omega)$, which is a complex number whose real and imaginary parts provide information on the elastic and the viscous nature of the material under investigation [56]. These are commonly indicated as the storage ($G'(\omega)$) and the loss ($G''(\omega)$) moduli, respectively. The conventional method of measuring the LVE properties of a material is based on the imposition of an oscillatory shear stress $\sigma(\omega, t) = \sigma_0 \sin(\omega t)$ (where σ_0 is the amplitude of the stress function) and the measurement of the resulting oscillatory shear strain, which would have a form like $\gamma(\omega, t) = \gamma_0(\omega) \sin(\omega t - \varphi(\omega))$, where $\gamma_0(\omega)$ and $\varphi(\omega)$ are the frequency-dependent strain amplitude and phase shift between the stress and the strain, respectively. The relationship between the shear complex modulus and the two experimental functions describing the stress and the strain is [56]:

$$G^*(\omega) = \frac{\hat{\sigma}(\omega)}{\hat{\gamma}(\omega)}, \tag{1}$$

where $\hat{\sigma}(\omega)$ and $\hat{\gamma}(\omega)$ are the Fourier transforms of $\sigma(\omega, t)$ and $\gamma(\omega, t)$, respectively. Notice that, equation 1 is of general validity; i.e., it applies to any temporal forms of the stress and the strain. In the particular case of sinusoidal

functions equation 1 returns:

$$G^*(\omega) = \frac{\sigma_0}{\gamma_0(\omega)}\cos(\varphi(\omega)) + \\ +i\frac{\sigma_0}{\gamma_0(\omega)}\sin(\varphi(\omega)) \equiv G'(\omega) + iG''(\omega), \tag{2}$$

which provides the expressions of the moduli as function of both the frequency-dependent functions $\gamma_0(\omega)$ and $\varphi(\omega)$. Notice that, $G^*(\omega)$ is time invariant [56].

Over the past century, the frequency behaviour of the viscoelastic moduli has been correlated, both theoretically and experimentally [56, 57, 58, 59], to the material's topological structure and molecular interactions at different length scales; i.e., from the bulk sample at relatively low frequencies, down to atomic length scales for frequencies of the order of THz. Hence, the importance of their knowledge over the widest possible range of frequencies to gain a full picture of the materials' structure and dynamics.

2.2. Passive Microrheology

When a micron-sized spherical particle is suspended in a fluid at thermal equilibrium, it experiences random forces leading to Brownian motion, driven by the thermal fluctuations of the fluid's molecules. Therefore, analysis of the particle's trajectory can reveal information on the viscoelastic properties of the suspending fluid, as demonstrated in the pioneering work of Mason and Weitz [20] that established the field of microrheology. In particular, they showed that the trajectory $\vec{r}(t)\ \forall\ t$ of a naturally buoyant bead is directly related to the LVE properties of the surrounding complex fluid by means of a generalised Langevin equation:

$$m\vec{a}(t) = \vec{f}_R(t) - \int_0^t \zeta(t-\tau)\vec{v}(\tau)d\tau \tag{3}$$

where m is the mass of the particle, $\vec{a}(t)$ is its acceleration, $\vec{v}(t)$ its velocity and $\vec{f}_R(t)$ is the usual Gaussian white noise term, modelling stochastic thermal forces acting on the particle. The integral term, which incorporates a generalised time-dependent memory function $\zeta(t)$, represents viscous damping by the fluid. Using the assumption that the Laplace-transformed bulk viscosity of the fluid

$\tilde{\eta}(s)$ is proportional to the microscopic memory function $\tilde{\zeta}(s) = 6\pi a\tilde{\eta}(s)$, where a is the bead radius, they provided the solution to equation (3) in terms of the particles' mean squared displacement (MSD):

$$G^*(\omega) = s\tilde{\eta}(s)|_{s=i\omega} = \frac{1}{6\pi a}\left[\frac{6k_BT}{i\omega\left\langle\Delta\widehat{r^2}(\omega)\right\rangle} + m\omega^2\right] \tag{4}$$

where k_B is Boltzmann's constant, T is absolute temperature and $\left\langle\Delta\widehat{r^2}(\omega)\right\rangle$ is the Fourier transform of the MSD, $\langle\Delta r^2(\tau)\rangle \equiv \left\langle[\vec{r}(t+\tau) - \vec{r}(t)]^2\right\rangle$. The average $\langle\ldots\rangle$ is taken over all initial times t and all particles, if more than one is observed.

2.3. The link between bulk and micro-rheology

Let us retrieve a straightforward relationship between the thermally driven MSD of a probe particle and the time-dependent shear compliance $J(t)$ of the suspending fluid. The latter (in conventional bulk-rheology) is defined as the ratio of the time-dependent shear strain $\gamma(t)$ to the magnitude σ_0 of the constant shear stress that is switched on at time $t = 0$:

$$J(t) = \gamma(t)/\sigma_0. \tag{5}$$

The compliance is related to the materials' shear relaxation modulus $G(t)$ by means of a convolution integral [56]:

$$\int_0^t G(\tau)\, J(t-\tau)\, d\tau = t. \tag{6}$$

Moreover, given that the complex shear modulus $G^*(\omega)$ is also defined as the Fourier transform of the time derivative of $G(t)$, by taking the Fourier transform of Eq. (6) one obtaines:

$$G^*(\omega) = i\omega\hat{G}(\omega) = \frac{1}{i\omega\hat{J}(\omega)}, \tag{7}$$

where $\hat{G}(\omega)$ and $\hat{J}(\omega)$ are the Fourier transforms of $G(t)$ and $J(t)$, respectively.

Moreover, given that the Fourier transform is a linear operator, by equating equations (7) and (4) one obtains:

$$\left\langle \Delta\widehat{r^2}(\omega) \right\rangle = \frac{k_B T}{\pi a} \hat{J}(\omega) \quad \Longleftrightarrow \quad \left\langle \Delta r^2(\tau) \right\rangle = \frac{k_B T}{\pi a} J(t), \tag{8}$$

where it has been assumed that for micron sized particles the inertial term $m\omega^2$ (otherwise present on the right side of equation (4)) is negligible for frequencies much smaller than MHz and that $J(0) = 0$ for viscoelastic fluids. Equation (8) expresses the linear relationship between the MSD of suspended spherical particles and the macroscopic creep compliance of the suspending fluid [60]. Therefore, it allows the evaluation of the fluid's complex shear modulus (*via* equation (4)) without the need of any preconceived model once an effective analytical method for performing the Fourier transform of a discrete set of experimental data is adopted, like either of the two methods discussed in Ref. ••[61].

3. Microrheology with Optical Tweezers (MOT)

3.1. OT calibration

Like any other mechanical transducer, also OT setups require to be calibrated to define their operational range in terms of *space*, *force* and *frequency* (or *time*).

3.1.1. Spatial calibration

In the case of OT equipped with a digital camera (as schematically shown in Figure 1), the spatial calibration process consists in correlating the pixel dimensions of an acquired image to the real dimensions of the captured features. This process can be easily performed by means of a calibration slide on which a metric scale bar is drawn. The average value of repeated measurements of the distance between two bars provides an accurate estimation of the pixel/unit conversion factor. Once the position detector is calibrated, then in order to measure a particle trajectory, an image analysis process is required. In the majority of the cases, home made routines are developed by the OT operators using a

variety of image analysis softwares. However, the basic principles underpinning the majority of particle tracking procedures have been clearly explained in the pioneering work of John C. Crocker and David G. Grier [62].

In the case of OT equipped with a quadrant photodiode (QPD) device, the spatial calibration is not straightforward as for the previous case and it is still a topic of study, reason for which I refer the reader to dedicated works [63, 64]•[65]. In brief, QPDs are discrete components consisting of four optically active areas separated by a small gap (of a few 10s of μm). In OT, a lens is positioned such that the back focal plane of the condenser is imaged onto the QPD (see Figure 1). Translations of the trapped particle in the laser focus causes translations of the laser spot in the back-focal plane, detected by the QPD. Some systems use a separate laser from that used to trap the object to monitor its position. In general, such systems have found applications in biophysics and colloidal science [66, 67].

3.1.2. Force calibration

One of the most important features of optical tweezers is that the confining action of an highly focussed laser beam exerted on a spherical particle can be modelled like a harmonic potential $E(\vec{r})$ of force constant κ:

$$E(\vec{r}) = \frac{1}{2}\kappa\langle r^2\rangle_{eq}, \tag{9}$$

where $\langle r^2\rangle_{eq}$ is the time-independent variance of the particle position from the trap centre, the origin of $\vec{r}$, at thermodynamic equilibrium. It follows that the restoring force exerted on the particle is simply given by the negative gradient of $E(\vec{r})$:

$$\vec{F} = -\nabla E(\vec{r}) = -\kappa\vec{r}. \tag{10}$$

In order to quantify the force exerted on the particle, a calibration of the elastic constant (trap stiffness) κ is thus necessary. This is simply achieved by appealing to the Principle of Equipartition of Energy, which in simple words states that at thermal equilibrium energy is shared equally among all of its

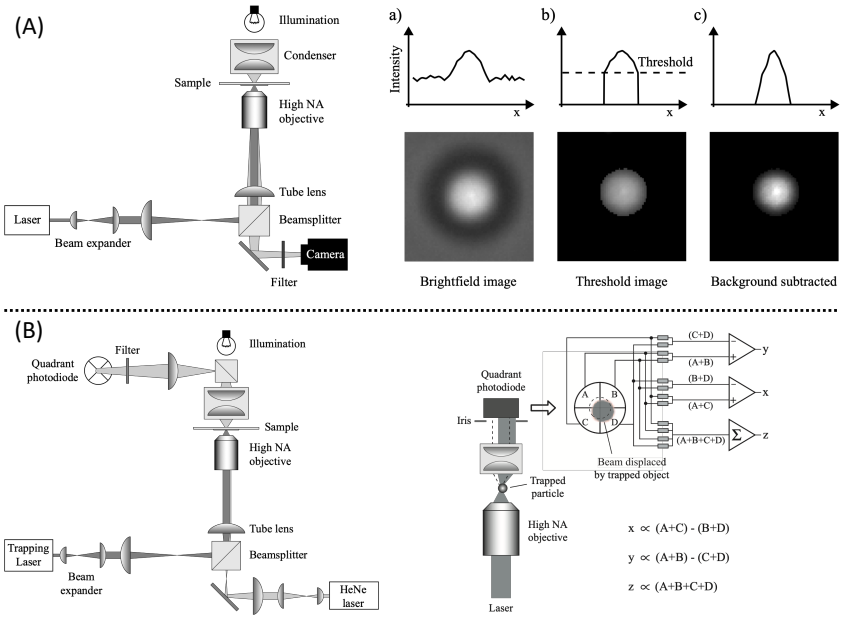

Figure 1: Two typical optical tweezers configurations. (A, left) A trapping laser beam is expanded to fill the aperture of a high numerical aperture microscope objective, coupled into an inverted microscope using a beamsplitter or suitable dichroic mirror. A tungsten-halogen lamp and condenser is used to illuminate the sample for viewing. The motion of trapped particles in the sample is analysed using a video camera. (A, right) Video tracking of a 2 μm silica bead, a) unprocessed bright field image; b) thresholded image; c) image with background subtracted. (B, left) A typical optical tweezers configuration equipped with a quadrant photodiode. A separate tracking laser is used to illuminate the sample. (B, right) A quadrant photodiode located in the back focal plane of the condenser lens can be used to measure the position of a trapped particle. A lateral displacement of the particle results in a lateral shift of the laser spot on the detector, creating a difference in the output signals from the differential amplifiers [47].

various forms; analytically this translates as:

$$\frac{d}{2}k_BT = \frac{1}{2}\kappa\langle r_j^2\rangle_{eq}, \tag{11}$$

where $\langle r_j^2\rangle$ is the Cartesian component ($j = x, y, z$) of the time-independent variance of the d-dimensional vector describing the particle's displacement from the trap centre ($\vec{r} = \vec{0}$, Figure 2). It is important to highlight that, for non-

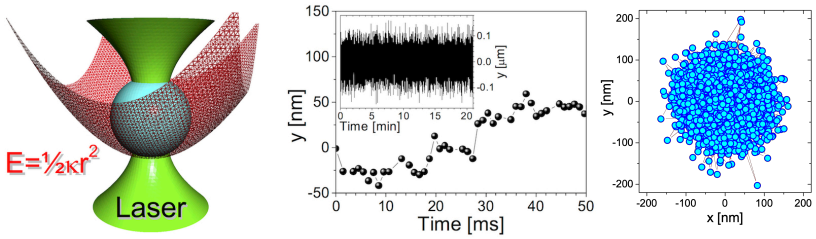

Figure 2: Optical Tweezers and particle trajectory. (Left) A schematic representation of an optically trapped bead within an harmonic potential $E(\vec{r})$, where κ and $\vec{r}$ are the trap stiffness and the bead position from the trap centre, respectively. (Middle) The y-component of the trajectory of an optically trapped bead of 2.5 μm radius suspended in water over a period of 50 ms. The inset shows the same component as before, but over the entire duration of the experiment of 22 min. (Right) The same data as before, plotted on the x, y-plane.

symmetric traps (i.e. $\kappa \neq \kappa_j, \forall j$) equation 11 is still valid, but only in one dimension, with κ replaced by κ_j evaluated for each direction:

$$k_B T = \kappa_j \langle r_j^2 \rangle_{eq}. \tag{12}$$

Despite the great variety of methods for determining the trap stiffness (e.g., using the power spectrum or the drag force [68, 69, 63]), equation 11 (or 12) provides the only such measurement that is independent of the viscoelastic properties of the fluid under investigation and is thus essential for microrheology studies. This is because, whatever the elasticity of the unknown fluid, its contribution to the time-independent constraining force must vanish at long times, because at rest the fluid's elastic shear modulus goes to zero as the time goes to infinity (or equivalently as the frequency goes to zero). Therefore, the trap stiffness is easily determined by means of equation 11 applied to a '*sufficiently long*' measurement; i.e., much longer than the longest characteristic relaxation time of the material under investigation, which for liquids is often identified by the low-frequency crossover of the moduli.

An alternative method for measuring the force acting on the particle, without any calibration of the spring constant of the optical trap, has been proposed by Farré *et al.* [70] by measuring the power and momentum distribution of light

that has passed through a trapped particle. However, the precise relationship between the power of a light beam and its force has been the subject of debate [71]; leaving equation 11 (or 12) yet the simplest and most efficient method.

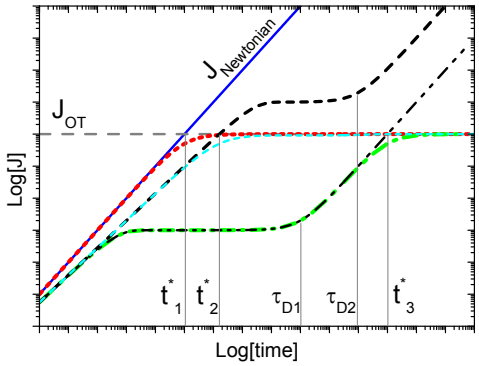

Figure 3: Double logarithmic schematic representation of a particle mean-square-displacement in terms of the creep compliance (see equation 8) suspended into both Newtonian and non-Newtonian fluids, with and without optical trapping. The abscissa values t^* and τ_D identify the longest relaxation-time of the viscoelastic fluid and the characteristic time of the compound system, respectively; the latter depends on the trap stiffness, the particle size and the complex fluid under investigation.

3.1.3. Temporal calibration

In general, in microrheological measurements with OT, the extremes of the experimental frequency window $[\omega_{min}, \omega_{max}]$ are defined at the higher end by the acquisition rate (AR) of the device detecting the particle position (i.e., $\omega_{max} = AR$, with $\omega_{max} \approx 10^3$ Hz or $\approx 10^5$ Hz depending on whether the setup is equipped with a camera or a QPD, respectively). The lowest accessible frequency (below which no useful rheological informations can be gained) depends on the trap stiffness, the particle size and the complex fluid under investigation; hence, its non-uniqueness. In particular, in the case of a static optical trap, it has been shown [52, 47] that ω_{min} can be identified in terms of a characteristic time ($t^* \approx 1/\omega_{min}$) at which the fluid compliance ($J(t) = t/\eta(t)$, where $\eta(t)$ is the viscosity of the fluid) equals that of the optical trap ($J_{OT} = 6\pi a/\kappa$):

$J(t^*) = J_{OT}$ (as schematically shown in Figure 3). The abscissa of the intercept between $J(t)$ and J_{OT} identifies t^*, whatever the viscoelastic nature of the suspending fluid. In the case of a Newtonian fluid with a time-independent viscosity η, the compliance is simply proportional to the time: $J(t) = t/\eta$ (which is represented by the continuous line of colour blue in Figure 3). It follows that the lowest accessible frequency is $\omega_{min} \simeq 1/t^* = \kappa/(6\pi a\eta)$, also known as the system's "*corner frequency*" [68]. Whereas, in the case of a non-Newtonian fluid, similar arguments as for the above case can be made, but the unknown temporal form of the compliance makes impossible to determine t^* *a priori*. Nonetheless, a good estimation of its value is achievable graphically from the abscissa of the intercept between $J(t)$ and J_{OT} (Figure 3). It is important to highlight that, for frequency values lower than ω_{min}, the compliance of the OT overshadows the one of the (viscoelastic) fluid and no useful rheological information can be obtained from the analysis of the data at times $t > t^*$. Hence, the need of lengthy measurements (i.e., of duration much longer than t^*) for an accurate calibration of the trap stiffness by means of either of the above mentioned equations 11 and 12.

3.2. Hybrid MOT

While the majority of microrheology techniques belong to either one of 'passive' or 'active' families, OT are the only such systems where an external force is always active onto the probe particle, whatever the chosen *modus operandi*; hence, its '*hybrid nature*'. In particular, in the case of passive MOT, where both the trap position and stiffness are time-invariant, the particle is subject to a *weak* restoring force that confines in space its thermally driven Brownian motion. Nonetheless, the latter can still be analysed by means of the same statistical mechanics principles adopted to investigate the trajectories of freely diffusing particles [20], as elucidated in section 3.2.1. On the other hand, in the case of active MOT, experiments are designed such that a relatively *strong* force is applied to induce a particle displacement of magnitude significantly bigger

than the thermal fluctuations (induced by the molecules of the surrounding media), which in this case turn to be an 'undesired noise' that disrupts the quality of the measurement, as expounded in section 3.2.2.

3.2.1. Passive MOT

When the particle's fluctuations are constrained by a stationary harmonic potential generated by optical tweezers, one could write a generalised Langevin equation similar to equation (3), but with an additional term accounting for the trapping force:

$$m\vec{a}(t) = \vec{f}_R(t) - \int_0^t \zeta(t-\tau)\vec{v}(\tau)d\tau - \kappa\vec{r}(t). \tag{13}$$

Following the same assumptions made by Mason & Weitz for the case of freely diffusing particles, equation (13) can be solved for the materials' complex modulus in terms of either the normalised mean squared displacement (NMSD) $\Pi(\tau) = \langle \Delta r^2(\tau) \rangle / 2 \left\langle r^2 \right\rangle$ [43] or the normalised position autocorrelation function (NPAF) $A(\tau) = \langle \vec{r}(t)\vec{r}(t+\tau) \rangle \,/\, \left\langle r^2 \right\rangle$ [44] (as shown in Figure 4):

$$G^*(\omega)\frac{6\pi a}{\kappa} = \left(\frac{1}{i\omega\hat{\Pi}(\omega)} - 1\right) \equiv \left(\frac{1}{i\omega\hat{A}(\omega)} - 1\right)^{-1} \equiv \frac{\hat{A}(\omega)}{\hat{\Pi}(\omega)} \tag{14}$$

where $\hat{\Pi}(\omega)$ and $\hat{A}(\omega)$ are the Fourier transforms of $\Pi(\tau)$ and $A(\tau)$, respectively. The inertial term ($m\omega^2$) present in the original works [43, 44] has been here neglected, because for micron-sized particles it only becomes significant at frequencies of the order of MHz. Moreover, for *sufficiently long* measurement, it is straightforward to demonstrate that $A(\tau)$ and $\Pi(\tau)$ are simply related to each other [44]:

$$\Pi(\tau) \equiv \frac{\left\langle r^2(t+\tau) \right\rangle + \left\langle r^2(t) \right\rangle - 2\left\langle \vec{r}(t_0)\vec{r}(\tau) \right\rangle}{2\left\langle r^2 \right\rangle} \equiv 1 - A(\tau) \tag{15}$$

In addition, by Fourier transforming equation (15) one obtains the relation: $i\omega\hat{\Pi}(\omega) = 1 - i\omega\hat{A}(\omega)$; hence the equivalences in equation (14).

At this point it is important to highlight that, while equation (13) is of general validity and it is applicable to any viscoelastic material (either liquid or

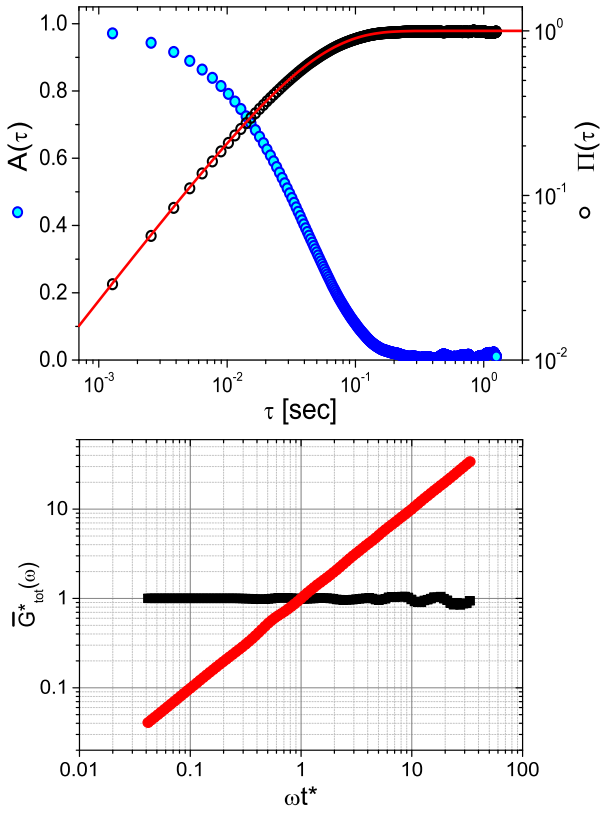

Figure 4: (Top) The normalised position autocorrelation function $A(\tau)$ and the normalised mean square displacement $\Pi(\tau)$ *versus* lag-time τ evaluated from the trajectory shown in Figure 1. The continuous line is the theoretical prediction: $\Pi(\tau) = 1 - A(\tau) = \left(1 - e^{-\tau/t^*}\right)$. (Bottom) The complex modulus *vs.* frequency (both normalised by $(6\pi a)/\kappa$ and $t^* = (6\pi a\eta)/\kappa$, respectively) evaluated *via* equation (14) and by means of equation (22) applied to either one of the data shown above, but interpolated with a natural cubic spline function and oversampled at $f_s = 25MHz$.

solid) to determine its complex modulus, without the need of any preconceived model to interpret the data, the same cannot be said for all those microrheology studies adopting a Langevin equation with a time invariant drag coefficient (i.e., $6\pi a\eta$, where η is a constant viscosity). Therefore, in order to avoid potentially misleading information, the latter approach should be employed *if and only if* the suspending 'fluid' is Newtonian. Similar arguments could be made when a

Lorentzian function is adopted to fit the power spectral density ($S(\omega)$) of the particle fluctuations; a procedure that is valid only for Newtonian fluids [68]. Moreover, even when attempts are made to derive the materials' viscoelastic properties directly from the analysis of $S(\omega)$, the use of predetermined fitting functions or Kramers–Kronig transformations are needed ••[61].

3.2.2. Active MOT

Active microrheology with OT is commonly performed via oscillatory measurements like the conventional bulk rheology method described by equations 1 and 2. However, in the case of MOT of *complex* fluids, the expression of $G^*(\omega)$ must be obtained via the solution of a generalised Langevin equation similar to equation 13, but with an extra term accounting for a non stationary trap:

$$m\vec{a}(t) = \vec{f}_R(t) - \int_0^t \zeta(t-\tau)\vec{v}(\tau)d\tau + \kappa\left(\vec{r}_c(t) - \vec{r}(t)\right), \tag{16}$$

where all the terms are the same as in equation 13 plus $\vec{r}_c(t)$ that is the position vector describing the driven motion of the optical trap center. Equation 16 can be solved for $G^*(\omega)$ in terms of the particle position $\vec{r}(t)$ and the resulting expression is [72]:

$$G^*(\omega)\frac{6\pi a}{\kappa} = \left(\frac{\langle\hat{r}_c(\omega)\rangle}{\langle\hat{r}(\omega)\rangle} - 1 + \frac{m\omega^2}{\kappa}\right) \cong \frac{\hat{r}_c(\omega)}{\widehat{\langle r\rangle}(\omega)} - 1 \tag{17}$$

where $\hat{r}_c(\omega)$ and $\hat{r}(\omega)$ are the Fourier transforms of $\vec{r}_c(t)$ and $\vec{r}(t)$, respectively. The brackets $\langle ... \rangle$ denote the average over *several* independent measurements. For the last equality it has been considered that: (i) $\langle\hat{r}_c(\omega)\rangle \equiv \hat{r}_c(\omega)$, being the latter the driving component, thus reproducible over several independent measurements, (ii) $\langle\hat{r}(\omega)\rangle \equiv \widehat{\langle r\rangle}(\omega)$ because of linearity of the involved operators, (iii) the particle inertia is negligible. Notice that, equation 17 is of general validity, whatever is the temporal form of $\vec{r}_c(t)$.

In the simplest case, when the optical trap is periodically oscillating with a driving frequency β, i.e. $\vec{r}_c(t) = \|r_c\| sin(\beta t)$, the particle displacement will assume a temporal form like $\vec{r}(t) = \|r\| sin(\beta t - \varphi(\beta))$; where $\|r_c\|$ and $\|r\|$ are

the amplitudes of the sinusoidal functions $\vec{r}_c(t)$ and $\vec{r}(t)$, respectively. Therefore, equation 17 simplifies [72]:

$$G^*(\beta)\frac{6\pi a}{\kappa} = \frac{\|r_c\|}{\|\langle r\rangle\|}e^{i\varphi(\beta)\beta} - 1, \tag{18}$$

from which the viscoelastic moduli assume the following expressions:

$$G'(\beta)\frac{6\pi a}{\kappa} = \frac{\|r_c\|}{\|\langle r\rangle\|}\cos(\varphi(\beta)) - 1 \tag{19}$$

$$G''(\beta)\frac{6\pi a}{\kappa} = \frac{\|r_c\|}{\|\langle r\rangle\|}\sin(\varphi(\beta)). \tag{20}$$

The above equations are similar to those obtained by others [45], but in Ref. [72] they have been derived rigorously. Moreover, it is important to highlight that, in order to obtain an accurate estimation of the moduli (i.e., of both the phase shift $\varphi(\beta)$ and the amplitude $\|\langle r\rangle\|$), for *each* explored frequency β, *several* cycles must be repeated to average out the thermal fluctuations that disrupt the particle trajectory. Therefore, in order to measure $G^*(\omega)$ over a wide frequency spectrum (e.g., from 0.01 Hz to kHz) a total measurement duration T_m of the order of *hours* would be required.

An alternative and *less time-consuming* method than the oscillatory measurements has been presented by Preece *et al.* [44] They introduced a *self-consistent* procedure for measuring the LVE properties of materials across the *widest* frequency range achievable with optical tweezers, by combining both passive and active OT operating modes. In particular, their procedure consists of two steps: (I) measuring the thermal fluctuations of a trapped bead for a sufficiently long time; (II) measuring the transient displacement of a bead flipping between two optical traps (spaced at fixed distance $D_0 \leqslant 0.8a$, to ensure the linearity of the optical trap [73]) that alternately switch on/off at a *sufficiently low* frequency (to allow a complete migration of the particle, as shown in Figure 5). The analysis of the first step (I) provides: (a) the traps stiffness (κ_i, $i = 1, 2$; by means of equation 11) — note that this has the added advantage of making the method self-calibrated — and (b) the high frequency viscoelastic properties of the material, to a high accuracy (by means of equation 14). The

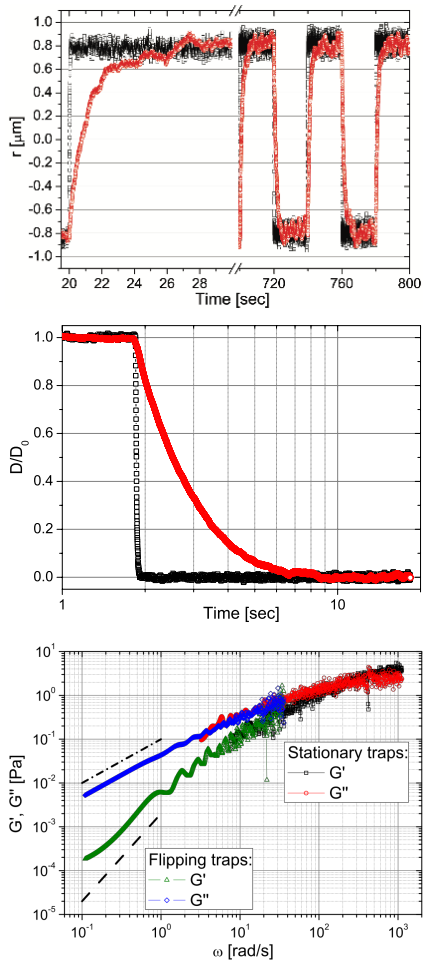

Figure 5: (Top) The trajectory of a $5\mu m$ diameter bead flipping between two optical traps at $r \simeq -0.8$ μm and $r \simeq 0.8$ μm repeatedly switching after a duration $P = 20$ s. The bead is suspended in (squares) water (with $\kappa_1 = 2.7$ and $\kappa_2 = 2.5$ μN/m) and (circles) a water-based solution of PAM at concentrations of 1 % w/w (with $\kappa_1 = 2.1$ and $\kappa_2 = 2.2$ μN/m). (Middle) The normalised mean position of all step-down data shown above; i.e., when simultaneously trap 2 (top) switches *off* and trap 1 (bottom) switches *on*. (Bottom) The complex moduli *vs.* frequency evaluated by combining the results obtained from a stationary trap (by means of equation 14) and two flipping traps (via equation 21 applied to the measurements shown above). Notice that, the presence of an overlapping region of the moduli makes the overall procedure self-consistent. Images reproduced with permission from Ref. [44].

second step (II) has the potential to provide information about the material's viscoelastic properties over a very wide frequency range, which is only limited (at the top end) by the acquisition rate of the bead position and (at the bottom end) by the duration (P) of the on/off state of the two traps. The latter procedure consists of analysing the bead's transient displacements as it moves between two traps with separation D_0 that swap their on/off state at times $t = t_0 + nP$. Preece *et al.* defined the normalised mean position of the particle as $D(t) = |\langle \vec{r}(t) \rangle| / D_0$, where the brackets $\langle ... \rangle$ denote the average over *several* independent measurements, but not over absolute time, since time-translation invariance is broken by the periodic switching. In the simple case of two identical optical traps ($\kappa_1 \equiv \kappa_2$) and particle inertia negligible, the expression of the fluid's complex modulus is:

$$G^*(\omega)\frac{6\pi a}{\kappa} = \frac{i\omega\hat{D}(\omega)}{\left(1 - i\omega\hat{D}(\omega)\right)}, \tag{21}$$

where $\hat{D}(\omega)$ is the Fourier transform of $D(t)$, with $\vec{r}(t)$ being the particle position from the active trap (i.e., $\vec{r}(t_0 + nP) \cong D_0$). The full viscoelastic spectrum of the fluid is resolved by combining the results obtained from steps (I) and (II).

3.2.3. Fourier transform of a discrete set of data

In principle, equations (4), (14), (17) and (21) are simple expressions relating the material's complex shear modulus $G^*(\omega)$ to the observed time-dependent bead trajectory $\vec{r}(t)$ via the Fourier transform of one of the related time-averaged quantities. In practice, it has been shown [52] ••[61] that the evaluation of the Fourier transform of a sampled function, given only a finite set of data points over a finite time domain, is non-trivial [20, 74, 75] since interpolation and extrapolation from those data can yield artefacts that lie within the bandwidth of interest.

An analytical procedure for the evaluation of the Fourier transform of any generic function sampled over a finite time window was proposed by Evans *et al.* [76, 77], to convert $J(t)$ into $G^*(\omega)$ directly (i.e., via equations (7)), without

the use of Laplace transforms or fitting functions. This method is based on the interpolation of the finite data set by means of a piecewise-linear function. In particular, the general validity of the proposed procedure makes it equally applicable to find the Fourier transform $\hat{g}(\omega)$ of any time-dependent function $g(t)$ that vanishes for negative t, sampled at a finite set of data points (t_k, g_k), where $k = 1 \dots N$, which extend over a finite range, and *need not* be equally spaced [76]:

$$-\omega^2 \hat{g}\left(\omega\right) = i\omega g(0) + \left(1 - e^{-i\omega t_1}\right) \frac{\left(g_1 - g(0)\right)}{t_1} + \\ + \dot{g}_\infty e^{-i\omega t_N} + \sum_{k=2}^{N} \left(\frac{g_k - g_{k-1}}{t_k - t_{k-1}}\right) \left(e^{-i\omega t_{k-1}} - e^{-i\omega t_k}\right) \tag{22}$$

where $\dot{g}_\infty$ is the gradient of $g(t)$ extrapolated to infinite time and $g(0)$ is the value of $g(t)$ extrapolated to $t = 0$ from above.

The above method was improved by Tassieri *et al.* [52] while analysing microrheology measurements performed with optical tweezers and its effectiveness has been corroborated by direct comparison with conventional bulk-rheology measurements of a variety of complex fluids [78, 79]. The authors [52] found that a substantial reduction in the size of the high-frequency artefacts, from which some high-frequency noise tends to spill over into the top of the experimental frequency range, can be achieved by an *over-sampling* technique. The technique involves first numerically interpolating between data points using a standard non-overshooting cubic spline, and then generating a new, over-sampled data set, by sampling the interpolating function not only at the exact data points but also at a number of equally-spaced points in between. Notice that, over-sampling is a common procedure in signal processing and it consists of sampling a signal with a sampling frequency f_s much higher than the Nyquist rate $2B$, where B is the highest frequency contained in the original signal. A signal is said to be oversampled by a factor of $\beta \equiv f_s/(2B)$ [80].

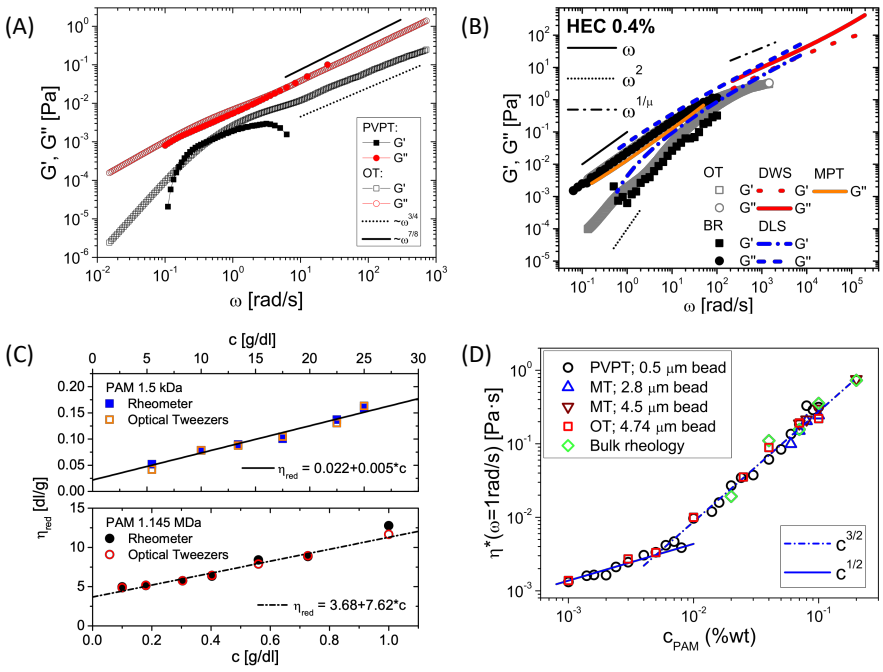

Figure 6: (A) Comparison between the complex moduli *vs.* frequency evaluated by means of both OT [52] and passive video particle tracking (PVPT) [84] of a solution of F-actin at a concentration of 0.1 mg/ml. (B) Comparison between the hydroxyethyl cellulose (HEC) solutions' linear viscoelastic moduli *vs.* frequency measured by means of conventional rotational rheometry (BR), optical tweezers (OT), diffusive wave spectroscopy (DWS), dynamic light scattering (DLS) and multiple particle tracking (MPT), for an HEC solution having concentration of 0.4 wt% (image reproduced with permission from Ref. [34]); where $\mu = 1.76$ [58, 85]. (C) Comparison between the reduced viscosity (η_{red}) *vs.* concentration measured by means of both OT and conventional rotational rheometry of water-based solutions of two polyacrylamides (PAM) having molecular weights of 1.5 kDa (top) and 1.145 MDa (bottom). Lines are the best linear fits of OT data. The linear extrapolation of η_{red} to zero concentration provides a reading of the PAMs' intrinsic viscosities (image reproduced with permission from Ref. [27]). (D) Comparison between the complex viscosity ($\eta^*(\omega) = G^*(\omega)/i\omega$) evaluated at $\omega = 1$ *vs.* concentration measured by means of conventional rotational rheometry, optical tweezers (OT), magnetic tweezers (MT), and passive video particle tracking (PVPT) of water-based solutions of PAM having molecular weight of 18 MDa [84]. In (A), (B) and (D) lines are guides for the gradients.

4. Bulk *vs.* Micro

One of the most popular *dilemmas* when performing microrheology measurements is whether their results provide a reliable representation of the materials' bulk rheology properties; given the significant difference in length scales at which measurements are performed (i.e., μm *vs.* cm, respectively). This indeed is a critical question that underpins the reliability of linear microrheology outcomes depending on whether or not the following two conditions are fulfilled (when of course non-linear [81] and inertia [82] effects or material's related issues such as aging, evaporation, and mutational effects [83] have been already pondered): (i) the material under investigation must appear homogeneous and/or isotropic at length scales much smaller than the characteristic dimension of the probe particle (e.g., in the case of solutions of semi-flexible polymers, the bead diameter must be bigger than the average mash size of the polymer network [22, 23, 24, 28]); (ii) microrheology measurements must be statistically valid, which experimentally translates either in measurements with a sufficiently long time of duration (T_m) (e.g., in the case of OT, $T_m \gg t^*$ for a proper calibration of the trap stiffness) or a big number of tracer particles homogeneously distributed within the sample. The satisfaction of both the above mentioned conditions would grant a good agreement between conventional bulk rheology and microrheology measurements as corroborated by the results reproduced in Fig. 6, where rheological parameters obtained from different microrheology techniques, such as optical tweezers, diffusive wave spectroscopy, dynamic light scattering, magnetic tweezers, multiple particle tracking and bulk rheology measurements are compared for five different materials.

5. MOT of living organisms

When microrheology measurements are attempted in living organisms (e.g., cells or parasites), attention must be paid to the characteristic time-scales involved in the experiments. This is because the mechanical properties of the organisms

may not be considered *time-invariant* for all the explored times. In particular, it has been shown [30, 86, 87] that the presence of "*athermal*" fluctuations within a living cell, due to the existence of active processes (e.g., actin-myosin interactions [88]) that dissipate energy not just by simple friction, drives the system out of thermodynamic equilibrium. Therefore, their existence should not be neglected as they may alter significantly the viscoelastic response of the system (mostly at low frequencies), with the risk of gathering deceptive information. The evaluation of the error carried by such negligence is not trivial as different organisms may dissipate energy in different ways and time-scales. Moreover, *athermal* processes are expected [30, 86, 87, 88] to occur within a range of frequency spanning from 10^{-2} Hz to 10^{2} Hz, with rate values that may vary even within the same population of organisms. From a microrheology point of view, one could consider the fastest rate (Γ_{org}) of all the *athermal* biological process occurring within an organism as the lowest frequency limit for the applicability of the fluctuation–dissipation theorem [89], which underpins the field of microrheology by linking the particle motion to the viscoelastic nature of the suspending medium [20].

It follows that, microrheology of living organisms could still be performed if the right assumptions on the *time-scales* involved during the measurement are made; i.e., on the Deborah number [90]. This is defined as the ratio between the characteristic relaxation time of the system under study and the time spent to observe it:

$$De = \frac{time\ of\ relaxation}{time\ of\ observation}. \tag{23}$$

Therefore, for each living organism, one could assume the existence of a characteristic time ($\tau_{org} = \Gamma_{org}^{-1}$) such that, for measurements having duration T_m shorter than τ_{org} (i.e., $De \gtrsim 1$) the living system can be seen as a complex material (either *fluid* or *solid*) with *time-invariant* viscoelastic properties. Whereas, for observations lasting longer than τ_{org} (i.e., $De \lesssim 1$), the living organism has time to self-reorganise and to move out of thermodynamic equilibrium.

In the case of MOT, it has been shown that for an accurate evaluation of

the relevant time-averaged functions (e.g., $\langle r^2 \rangle$, $\Pi(\tau)$, $A(\tau)$, $D(t)$ or the MSD) *sufficiently long* measurements are required (i.e., of the order of *tens* of minutes). Therefore, this would very likely result in $De \lesssim 1$ for a great majority of living organisms, with the lost of the pseudo-equilibrium assumption due to the start of *athermal* processes within the system. Thus, the potential inappropriateness of OT for measuring the linear viscoelastic properties of living systems [72].

6. Conclusions

Optical tweezers have been used in a variety of scientific contexts, across the physical and life sciences. Fields as diverse as statistical mechanics and molecular biology have benefit from the precise transduction of very small forces and displacements; establishing optical tweezers as an ideal tool for such purposes. The continuous development of optical trapping technologies has allowed the study of fundamental physics' principles and addressed both biological and chemical problems. As in microrheology, optical tweezers are maturing as a reliable technology and there is plenty of new opportunities for using these tools to gain a better understanding of yet unexplored processes occurring at microscopic length-scales.

7. Acknowledgments

I thank Miles Padgett, Jonathan Cooper, Graham Gibson, Mike Evans, Francesco Del Giudice, Amanda Wright, Michael Lee, Daryl Preece and Francesca Tassieri for helpful conversations. I acknowledge support via EPSRC grant (EP/R035067/1 – EP/R035563/1 – EP/R035156/1)

References

[1] A. Ashkin, Acceleration and trapping of particles by radiation pressure, Phys. Rev. Lett. 24 (4) (1970) 156–159.

[2] A. Ashkin, J. M. Dziedzic, Optical levitation by radiation pressure, Applied Physics Letters 19 (8) (1971) 283–285. doi:{10.1063/1.1653919}.

[3] A. Ashkin, J. M. Dziedzic, J. E. Bjorkholm, S. Chu, Observation of a single-beam gradient force optical trap for dielectric particles, Opt. Lett. 11 (5) (1986) 288–290.

[4] K. Svoboda, S. Block, Biological applications of optical forces, Annual Review of Biophysics and Biomolecular Structure 23 (1994) 247–285.

[5] R. Diekmann, D. L. Wolfson, C. Spahn, M. Heilemann, M. Schüttpelz, T. Huser, Nanoscopy of bacterial cells immobilized by holographic optical tweezers, Nature communications 7 (2016) 13711. The authors have adopted holographic optical tweezers to achieve, for the first time, super-resolution far-field fluorescence microscopy of non-adherent bacterial cells.

[6] J. F. Davies, K. R. Wilson, Raman spectroscopy of isotopic water diffusion in ultraviscous, glassy, and gel states in aerosol by use of optical tweezers, Analytical Chemistry 88 (4) (2016) 2361–2366. doi:10.1021/acs.analchem.5b04315. The authors have adopted optical tweezers to perform Raman spectroscopy of isotopic water diffusion in ultraviscous, glassy, and gel states in aerosol. The proposed method allows a simple and relatively quick (i.e., hours instead of days) yet accurate measurement of the diffusion coefficient of water.

[7] Y. A. Ayala, B. Pontes, D. S. Ether, L. B. Pires, G. R. Araujo, S. Frases, L. F. Romão, M. Farina, V. Moura-Neto, N. B. Viana, et al., Rheological properties of cells measured by optical tweezers, BMC biophysics 9 (1) (2016) 5. The authors introduce new method to investigate the rheological behaviour of fibroblasts, neurons and astrocytes in the frequency range from 1Hz to 35Hz. The method solves the combined action on a cell of an optical force and the induced displacement of a moving stage.

[8] W. Weigand, A. Messmore, J. Tu, A. Morales-Sanz, D. Blair, D. Deheyn, J. Urbach, R. Robertson-Anderson, Active microrheology determines

scale-dependent material properties of chaetopterus mucus, PloS one 12 (5) (2017) e0176732. The authors have adopted optical tweezers to investigate the rheological properties of *Chaetopterus* mucus. The outcomes reveal that mucus responds as a hierarchical network with a loose biopolymer mesh coupled to a larger scaffold responsible for macroscopic gel-like mechanics.

[9] H. Kim, W. Lee, H.-g. Lee, H. Jo, Y. Song, J. Ahn, In situ single-atom array synthesis using dynamic holographic optical tweezers, Nature communications 7 (2016) 13317. The authors have adopted holographic optical tweezers to generate high-fidelity atom-arrays for potential use in real-time qubit shuttling in high-dimensional quantum computing architectures.

[10] F. Pierini, K. Zembrzycki, P. Nakielski, S. Pawłowska, T. Kowalewski, Atomic force microscopy combined with optical tweezers (afm/ot), Measurement Science and Technology 27 (2) (2016) 025904. The authors present a new instrument that combines atomic force microscopy and optical tweezers. The augmented sensitivity of the proposed setup makes it a valuable option for nanomechanics, molecules manipulation and biological studies.

[11] X. Li, C. C. Cheah, A simple trapping and manipulation method of biological cell using robot-assisted optical tweezers: Singular perturbation approach, IEEE Transactions on Industrial Electronics 64 (2) (2017) 1656–1663. The authors present a simple tracking control method for optical manipulation that enables the laser beam to automatically trap and manipulate a cell, without high-order derivatives or construction of observers.

[12] Y. Yuan, Y. Lin, B. Gu, N. Panwar, S. C. Tjin, J. Song, J. Qu, K.-T. Yong, Optical trapping-assisted sers platform for chemical and biosensing applications: Design perspectives, Coordination Chemistry Reviews 339 (2017) 138–152. The authors present a comprehensive review on the systematic classification of optical trapping-assisted sensing platform for surface-enhanced Raman scattering and discuss its applications in biosens-

ing, bioimaging, chemical monitoring, particle manipulation, single cell analysis, *etc*.

[13] M. Donato, A. Mazzulla, P. Pagliusi, A. Magazzù, R. Hernandez, C. Provenzano, P. Gucciardi, O. Maragò, G. Cipparrone, Light-induced rotations of chiral birefringent microparticles in optical tweezers, Scientific reports 6 (2016) 31977. The authors present a study on the rotational dynamics of solid chiral and birefringent microparticles induced by elliptically polarized laser light in optical tweezers. This achievement paves the way to a wider range of optical control of the mechanical interaction between light and matter at the mesoscale.

[14] I. A. Favre-Bulle, A. B. Stilgoe, H. Rubinsztein-Dunlop, E. K. Scott, Optical trapping of otoliths drives vestibular behaviours in larval zebrafish, Nature Communications 8 (1). doi:10.1038/s41467-017-00713-2. The authors have adopted optical tweezers for in vivo manipulation of 55-micron otoliths in larval zebrafish. They have corroborated that OT are sufficiently powerful and precise tools to move large objects in vivo, and set the stage for the functional mapping of the resulting vestibular processing.

[15] L. Gardini, A. Tempestini, F. Pavone, M. Capitanio, High-speed optical tweezers for the study of single molecular motors, in: Molecular Motors, Springer, 2018, pp. 151–184. The authors provide a step-by-step protocol for the optimisation of optical tweezers setups to perform ultrafast force-clamp spectroscopy of myosin motors.

[16] R. Agrawal, T. Smart, J. Nobre-Cardoso, C. Richards, R. Bhatnagar, A. Tufail, D. Shima, P. H. Jones, C. Pavesio, Assessment of red blood cell deformability in type 2 diabetes mellitus and diabetic retinopathy by dual optical tweezers stretching technique, Scientific reports 6 (2016) 15873. The authors successfully corroborated the use of a dual optical tweezers configuration to investigate the deformability of red blood cells in type 2 diabetes mellitus without and with diabetic retinopathy.

[17] D. Strehle, P. Mollenkopf, M. Glaser, T. Golde, C. Schuldt, J. A. Käs, J. Schnauß, Single actin bundle rheology, Molecules 22 (10) (2017) 1804. The authors have developed a new method based on optical tweezers to determine the bending stiffness of individual bundles of actin filaments. This novel approach allows to systematically test anisotropic bundled structures, which play an essential role in the mechanical response of eukaryotic cells.

[18] Z. Mártonfalvi, P. Bianco, K. Naftz, G. G. Ferenczy, M. Kellermayer, Force generation by titin folding, Protein Science 26 (7) (2017) 1380–1390. The authors have adopted a high?resolution optical tweezers setup to gain new insights on the force?dependent folding/unfolding mechanisms of titin's globular domains.

[19] K. D. Whitley, M. J. Comstock, Y. R. Chemla, High-resolution "fleezers": Dual-trap optical tweezers combined with single-molecule fluorescence detection, in: Optical Tweezers, Springer, 2017, pp. 183–256. The authors describe a hybrid instrument that combine a high-resolution optical trap with a confocal fluorescence microscope, which can simultaneously detect sub-nanometer displacements, sub-piconewton forces, and single-molecule fluorescence signals.

[20] T. Mason, D. Weitz, Optical measurements of frequency-dependent linear viscoelastic moduli of complex fluids, Physical Review Letters 74 (7) (1995) 1250–1253. doi:{10.1103/PhysRevLett.74.1250}.

[21] T. M. Squires, T. G. Mason, Fluid Mechanics of Microrheology, Annual review of fluid mechanics 42 (2010) 413–438. doi:{10.1146/annurev-fluid-121108-145608}.

[22] M. Tassieri, T. Waigh, J. Trinick, A. Aggeli, R. Evans, Analysis of the linear viscoelasticity of polyelectrolytes by magnetic microrheometry-Pulsed creep experiments and the one particle response, Journal of rheology 54 (1) (2010) 117–131. doi:{10.1122/1.3266946}.

[23] M. Tassieri, R. Evans, L. Barbu-Tudoran, J. Trinick, T. Waigh, The self-assembly, elasticity, and dynamics of cardiac thin filaments, Biophysical journal 94 (6) (2008) 2170–2178. doi:{10.1529/biophysj.107.116087}.

[24] M. Tassieri, R. Evans, L. Barbu-Tudoran, G. N. Khaname, J. Trinick, T. A. Waigh, Dynamics of Semiflexible Polymer Solutions in the Highly Entangled Regime, Physical Review Letters 101 (19) (2008) 198301. doi:{10.1103/PhysRevLett.101.198301}.

[25] F. Watts, L. E. Tan, C. G. Wilson, J. M. Girkin, M. Tassieri, A. J. Wright, Investigating the micro-rheology of the vitreous humor using an optically trapped local probe, Journal of Optics 16 (1). doi:{10.1088/2040-8978/16/1/015301}.

[26] E. J. Robertson, G. Najjuka, M. A. Rolfes, A. Akampurira, N. Jain, J. Anantharanjit, M. von Hohenberg, M. Tassieri, A. Carlsson, D. B. Meya, T. S. Harrison, B. C. Fries, D. R. Boulware, T. Bicanic, Cryptococcus neoformans Ex Vivo Capsule Size Is Associated With Intracranial Pressure and Host Immune Response in HIV-associated Cryptococcal Meningitis, Journal of Infectious Diseases 209 (1) (2014) 74–82. doi:{10.1093/infdis/jit435}.

[27] M. Tassieri, F. Del Giudice, E. J. Robertson, N. Jain, B. Fries, R. Wilson, A. Glidle, F. Greco, P. A. Netti, P. L. Maffettone, et al., Microrheology with optical tweezers: Measuring the relative viscosity of solutions '*at a glance*', Scientific Reports 5 (2015) 8831.

[28] M. Tassieri, Dynamics of semiflexible polymer solutions in the tightly entangled concentration regime, Macromolecules 50 (14) (2017) 5611–5618.

[29] P. Kollmannsberger, B. Fabry, Linear and Nonlinear Rheology of Living Cells, Annual Review of Materials Research 41 (2011) 75–97. doi:{10.1146/annurev-matsci-062910-100351}.

[30] A. W. Harrison, D. A. Kenwright, T. A. Waigh, P. G. Woodman, V. J. Allan, Modes of correlated angular motion in live cells across three distinct time scales, Physical biology 10 (3). doi:{10.1088/1478-3975/10/3/036002}.

[31] S. Kuo, J. Gelles, E. Steuer, M. Sheetz, A model for kinesin movement from nanometer-level movements of kinesin and cytoplasmic dynein and force measurements, Journal of cell Science Supplement (14) (1991) 135–138, workshop on motor proteins, Cambridge, England, SEP, 1990.

[32] D. Pine, D. Weitz, P. Chaikin, E. Herbolzheimer, Diffusing-wave spectroscopy, Physical Review Letters 60 (12) (1988) 1134–1137. doi:{10.1103/PhysRevLett.60.1134}.

[33] D. Weitz, J. Zhu, D. Durian, H. Gang, D. Pine, Diffusing-wave spectroscopy - the technique and some applications, Physica scripta T49B (1993) 610–621. doi:{10.1088/0031-8949/1993/T49B/040}.

[34] F. Del Giudice, M. Tassieri, C. Oelschlaeger, A. Q. Shen, When microrheology, bulk rheology, and microfluidics meet: Broadband rheology of hydroxyethyl cellulose water solutions, Macromolecules 50 (7) (2017) 2951–2963.

[35] T. Garting, A. Stradner, Optical microrheology of protein solutions using tailored nanoparticles, Small (2018) 1801548.

[36] T. Okajima, H. Tokumoto, Nanorheology of living cells investigated by atomic force microscopy, Nihon reoroji gakkaishi 36 (2) (2008) 81–86. doi:{10.1678/rheology.36.81}.

[37] Y. H. Chim, L. M. Mason, N. Rath, M. F. Olson, M. Tassieri, H. Yin, A one-step procedure to probe the viscoelastic properties of cells by atomic force microscopy, Scientific reports 8 (1) (2018) 14462.

[38] A. Bausch, W. Moller, E. Sackmann, Measurement of local viscoelasticity and forces in living cells by magnetic tweezers, Biophysical journal 76 (1, Part 1) (1999) 573–579.

[39] R. Brau, J. Ferrer, H. Lee, C. Castro, B. Tam, P. Tarsa, P. Matsudaira, M. Boyce, R. Kamm, M. Lang, Passive and active microrheology with optical tweezers, Journal of optics A-pure and applied optics 9 (8, SI) (2007) S103–S112. doi:{10.1088/1464-4258/9/8/S01}.

[40] M. Fischer, K. Berg-Sorensen, Calibration of trapping force and response function of optical tweezers in viscoelastic media, Journal of optics A-pure and applied optics 9 (8, SI) (2007) S239–S250. doi:{10.1088/1464-4258/9/8/S18}.

[41] M. Atakhorrami, J. I. Sulkowska, K. M. Addas, G. H. Koenderink, J. X. Tang, A. J. Levine, F. C. MacKintosh, C. F. Schmidt, Correlated fluctuations of microparticles in viscoelastic solutions: Quantitative measurement of material properties by microrheology in the presence of optical traps, Physical Review E 73 (6, Part 1). doi:{10.1103/PhysRevE.73.061501}.

[42] A. Yao, M. Tassieri, M. Padgett, J. Cooper, Microrheology with optical tweezers, Lab on a Chip 9 (17) (2009) 2568–2575. doi:{10.1039/b907992k}.

[43] M. Tassieri, G. M. Gibson, R. Evans, A. M. Yao, R. Warren, M. J. Padgett, J. M. Cooper, Measuring storage and loss moduli using optical tweezers: Broadband microrheology, Physical Review E 81 (2, Part 2). doi:{10.1103/PhysRevE.81.026308}.

[44] D. Preece, R. Warren, R. Evans, G. M. Gibson, M. J. Padgett, J. M. Cooper, M. Tassieri, Optical tweezers: wideband microrheology, Journal of optics 13 (4, SI). doi:{10.1088/2040-8978/13/4/044022}.

[45] M. Valentine, L. Dewalt, H. OuYang, Forces on a colloidal particle in a polymer solution: A study using optical tweezers, Journal of physics-condensed matter 8 (47) (1996) 9477–9482, 3rd Liquid Matter Conference, Univ E Anglia, Norwich, England, JUL 06-10, 1996. doi:{10.1088/0953-8984/8/47/048}.

[46] L. Starrs, P. Bartlett, One- and two-point micro-rheology of viscoelastic media, Journal of physics-condensed matter 15 (1, SI) (2003) S251–S256, 5th Liquid Matter Conference, Constance, Germany, SEP 14-18, 2002. doi:{10.1088/0953-8984/15/1/333}.

[47] M. Tassieri, R. M. L. Evans, A. M. Yao, M. P. Lee, D. B. Phillips, G. M. Gibson, A. Baule, A. Papagiannopoulos, R. W. Bowman, Microrheology with Optical Tweezers: Principles and Applications, Pan Stanford, New York, 2015.

[48] T. A. Waigh, Microrheology of complex fluids, Reports on Progress in Physics 68 (3) (2005) 685.

[49] C. J. Pipe, G. H. McKinley, Microfluidic rheometry, Mechanics research communications 36 (1) (2009) 110–120. doi:{10.1016/j.mechrescom.2008.08.009}.

[50] P. Cicuta, A. M. Donald, Microrheology: a review of the method and applications, Soft Matter 3 (12) (2007) 1449–1455. doi:{10.1039/b706004c}.

[51] L. G. Rizzi, M. Tassieri, Microrheology of biological specimens, Encyclopedia of Analytical Chemistry.

[52] M. Tassieri, R. Evans, R. L. Warren, N. J. Bailey, J. M. Cooper, Microrheology with optical tweezers: data analysis, New Journal of Physics 14 (11) (2012) 115032.

[53] A. Pommella, V. Preziosi, S. Caserta, J. M. Cooper, S. Guido, M. Tassieri, Using Optical Tweezers for the Characterization of Polyelectrolyte Solutions with Very Low Viscoelasticity, Langmuir 29 (29) (2013) 9224–9230. doi:{10.1021/la4015948}.

[54] M. P. Lee, G. M. Gibson, D. Phillips, M. J. Padgett, M. Tassieri, Dynamic stereo microscopy for studying particle sedimentation, Optics Express 22 (4) (2014) 4671–4677. doi:{10.1364/OE.22.004671}.

[55] R. M. Robertson-Anderson, Optical tweezers microrheology: From the basics to advanced techniques and applications (2018).

[56] J. D. Ferry, Viscoelastic properties of polymers, 3rd Edition, Wiley, 1980.

[57] C. W. Macosko, R. G. Larson, Rheology: principles, measurements, and applications, VCH New York, 1994.

[58] M. Rubinstein, R. H. Colby, Polymer Physics, Oxford University Press: Oxford, 2003.

[59] T. McLeish, Tube theory of entangled polymer dynamics, Advances in Physics 51 (6) (2002) 1379–1527. doi:{10.1080/00018730210153216}.

[60] J. Xu, V. Viasnoff, D. Wirtz, Compliance of actin filament networks measured by particle-tracking microrheology and diffusing wave spectroscopy, Rheologica acta 37 (4) (1998) 387–398. doi:{10.1007/s003970050125}.

[61] M. Tassieri, Comment on "a symmetrical method to obtain shear moduli from microrheology" by k. nishi, m. l. kilfoil, c. f. schmidt, and f. c. mackintosh, soft matter, 2018, 14, 3716, Soft Matter 14 (42) (2018) 8666–8670. doi:10.1039/c8sm00806j. I corroborate the effectiveness of two analytical methods for performing the Fourier transform of any generic time-dependent function resembling the mean square displacement of an optically trapped bead; an essential mathematical process in microrheology with OT.

[62] J. Crocker, D. Grier, Methods of digital video microscopy for colloidal studies, Journal of colloid and interface science 179 (1) (1996) 298–310. doi:{10.1006/jcis.1996.0217}.

[63] S. F. Tolic-Norrelykke, E. Schaeffer, J. Howard, F. S. Pavone, F. Juelicher, H. Flyvbjerg, Calibration of optical tweezers with positional detection in the back focal plane, Review of Scientific Instruments 77 (10). doi:{10.1063/1.2356852}.

[64] S. Keen, J. Leach, G. Gibson, M. J. Padgett, Comparison of a high-speed camera and a quadrant detector for measuring displacements in optical tweezers, Journal of optics A-pure and applied optics 9 (8) (2007) S264–S266. doi:{10.1088/1464-4258/9/8/S21}.

[65] J. R. Staunton, B. Blehm, A. Devine, K. Tanner, In situ calibration of position detection in an optical trap for active microrheology in viscous materials, Optics express 25 (3) (2017) 1746–1761. The authors introduce a method for the calibration of optical tweezers equipped with a quadrant photodiode. The procedure consists in steering the detection laser beam while the probe is trapped.

[66] J. Finer, R. Simmons, J. Spudich, Single myosin molecule mechanics - piconewton forces and nanometer steps, Nature 368 (6467) (1994) 113–119. doi:{10.1038/368113a0}.

[67] J. Meiners, S. Quake, Direct measurement of hydrodynamic cross correlations between two particles in an external potential, Physical Review Letters 82 (10) (1999) 2211–2214. doi:{10.1103/PhysRevLett.82.2211}.

[68] K. Berg-Sørensen, H. Flyvbjerg, Power spectrum analysis for optical tweezers, Rev. Sci. Instrum. 75 (3) (2004) 594–612. doi:{10.1063/1.1645654}.

[69] K. Neuman, S. Block, Optical trapping, Review of scientific instruments 75 (9) (2004) 2787–2809. doi:{10.1063/1.1785844}.

[70] A. Farré, M. Montes-Usategui, A force detection technique for single-beam optical traps based on direct measurement of light momentum changes, Opt. Express 18 (11) (2010) 11955–11968. doi:10.1364/OE.18.011955.
URL http://www.opticsexpress.org/abstract.cfm?URI=oe-18-11-11955

[71] U. Leonhardt, Optics: Momentum in an uncertain light, Nature 444 (7121) (2006) 823–824.
URL http://dx.doi.org/10.1038/444823a

[72] M. Tassieri, Linear microrheology with optical tweezers of living cells 'is not an option'!, Soft Matter 11 (29) (2015) 5792–5798.

[73] A. Ashkin, Force of a single-beam gradient laser trap on a dielectric sphere in the ray optics regine, Biophysical journal 61 (2) (1992) 569–582.

[74] T. Mason, Estimating the viscoelastic moduli of complex fluids using the generalized Stokes-Einstein equation, Rheologica acta 39 (4) (2000) 371–378. doi:{10.1007/s003970000094}.

[75] B. Dasgupta, S. Tee, J. Crocker, B. Frisken, D. Weitz, Microrheology of polyethylene oxide using diffusing wave spectroscopy and single scattering, Physical Review E 65 (5, Part 1). doi:{10.1103/PhysRevE.65.051505}.

[76] R. M. L. Evans, M. Tassieri, D. Auhl, T. A. Waigh, Direct conversion of rheological compliance measurements into storage and loss moduli, Physical Review E 80 (1). doi:{10.1103/PhysRevE.80.012501}.

[77] R. M. L. Evans, Transforming from time to frequency without artefacts, British Society of Rheology Bulletin 50 (2009) 76. arXiv:0911.4652.
URL http://arxiv.org/abs/0911.4652

[78] M. Tassieri, M. Laurati, D. J. Curtis, D. W. Auhl, S. Coppola, A. Scalfati, K. Hawkins, P. R. Williams, J. M. Cooper, i-Rheo: Measuring the materials' linear viscoelastic properties "*in a step*"!, Journal of Rheology 60 (4) (2016) 649.

[79] M. Tassieri, J. Ramírez, N. C. Karayiannis, S. K. Sukumaran, Y. Masubuchi, i-rheo gt: Transforming from time to frequency domain without artifacts, Macromolecules 51 (14) (2018) 5055–5068.

[80] B. Lathi, Linear Systems and Signals, Oxford Series in Electrical and Computer Engineering, Oxford University Press, USA, 2004.
URL http://books.google.co.uk/books?id=7resQgAACAAJ

[81] Y. Jiang, T. Narushima, H. Okamoto, Nonlinear optical effects in trapping nanoparticles with femtosecond pulses, Nature Physics 6 (12) (2010) 1005.

[82] B. Lukić, Direct observation of nondiffusive motion of a brownian particle, Physical Review Letters 95 (16). doi:10.1103/PhysRevLett.95.160601.

[83] M. Mours, H. Winter, Time resolved rheometry, in: AitKadi, A and Dealy, JM and James, DF and Williams, MC (Ed.), XIITH International Congress on Rheology, Proceedings, 1996, pp. 737–738, XIIth International Congress on Rheology, Qiuebec City, Canada, AUG 18-23, 1996.

[84] M. Tassieri, Microrheology of semiflexible polymers, University of Leeds Ph.D. Thesis.

[85] R. H. Colby, Structure and linear viscoelasticity of flexible polymer solutions: comparison of polyelectrolyte and neutral polymer solutions, Rheologica Acta 49 (5) (2010) 425–442.

[86] D. Mizuno, C. Tardin, C. F. Schmidt, F. C. MacKintosh, Nonequilibrium mechanics of active cytoskeletal networks, Science 315 (5810) (2007) 370–373. doi:{10.1126/science.1134404}.

[87] T. Toyota, D. A. Head, C. F. Schmidt, D. Mizuno, Non-Gaussian athermal fluctuations in active gels, Soft Matter 7 (7) (2011) 3234–3239. doi:{10.1039/c0sm00925c}.

[88] B. Alberts, A. Johnson, J. Lewis, D. Morgan, M. Raff, K. Roberts, P. Walter, Molecular Biology of the Cell, Sixth Edition, Garland Science, 2015.

[89] Landau, L. D. and Lifshitz, E. M. and Pitaevskii, L. P., Statistical physics, 3d rev. and enl. ed Edition, no. 0080230393 (v. 1), Oxford ; New York : Pergamon Press, 1980.

[90] M. Reiner, The deborah number, Physics today 17 (1) (1964) 62.